Bioavailability of Ellagic Acid, Urolithin A and Urolithin B in Human Plasma after Pomegranate Juice or Extract Consumption

A thesis submitted by

Tianmeng Chen

In partial fulfillment of the requirements
for the degree of

Master of Science

In

Pharmacology and Drug Development

TUFTS UNIVERSITY

Sackler School of Graduate Biomedical Sciences

Date
May 22th, 2016
(Specify the actual month and year the degree will be awarded, not the date of your defense.)

Advisor:
Thesis Chair: Emmanuel Pothos
Project Mentor: David J. Greenblatt
Statistical Mentor: David J. Greenblatt

Abstract

Pomegranate products have been reported to have many beneficial effects including anti-oxidant, anti-inflammatory, and anti-proliferative properties. These health benefits are more likely to be attributed to the metabolites found after absorption rather than the intact components of pomegranate. To investigate the bioavailability of Ellagic Acid (EA), Urolithin-A (Uro-A), and Urolithin B (Uro-B), 12 healthy volunteers were administrated with 2 doses of pomegranate juice (PJ trial, ~800mg polyphenol/dose) or pomegranate extract (PE trial, ~689mg polyphenol/dose), and blood samples were collected at various time points for up to 12.5 hours after dosage. Protein precipitation by acetonitrile in an acidic environment was used for plasma extraction. Free and conjugated metabolites were both analyzed by comparing incubation and non-incubation with β-deglucuronidase. Because matrix effect varied among different individuals and could not be completely eliminated, matrix-matched calibration curve was adopted for analytical quantification. In volunteer no.3, free EA was detected in both PE and PJ trials, fast absorbed and quickly eliminated with T_{max} of ~1hr and AUC of ~57 (ng·h)/ml after administration. C_{max} for EA in PE and PJ trials were different: 25.0ng/ml in PE trial vs. 15.2ng/ml in PJ trial. For Uro-A, neither free nor glucuronide conjugated Uro-A were detectable in PE trial, but high concentrations of Uro-A glucuronide were detected in PJ trial. T_{max} for Uro-A would occur at least 12.5 hours later after consumption. Uro-B were undetectable in both trials. The evaluation of the pharmacokinetic profiles of target analytes in other subjects is still in process.

Acknowledgements

I would first like to thank my thesis advisor Dr. Greenblatt for his guidance, help and support. The door of his office was always open, whenever I had a question about my project. He always provided me with the necessary knowledge and valuable advice to guarantee my experiments in the right direction. I also really appreciated his word-by-word review for my master thesis.

Besides my advisor, I would like to thank Dr. Chen in Tufts Nutrition Center. He provided me many suggestions on using LC-MS and helped me to deal with the problem of matrix effect.

I would also like to thank Dr. Castellot for his guidance during my 2nd lab rotation, and to thank Dr. Beinfeld for her being my 2nd reviewer for my master thesis. I would like to thank Dr. Greenblatt, Dr. Castellot, and Dr. Beinfeld once again, for their full support during my Ph.D. application.

In addition, I would like to thank all the co-workers in our lab, especially Yuli and Lei who always gave me a hand when I was facing some difficulties in my project.

Finally, I would like to express my gratitude to my parents from the bottom of my heart, for their unconditional support and continuous encouragement.

Thank you so much, everyone!

Tianmeng

Table of Contents

List of Tables

List of Figures

List of Abbreviations

A. ETs: ellagitannins

B. EA: ellagic acid

C. Uro-A: urolithin A

D. Uro-B: urolithin B

E. LC: liquid chromatography

F. MS: mass spectrometry,

G. MF: matrix factor

H. ME: matrix effect

I. RE: recovery of extraction

J. PE: process efficiency

K. C_{max}: the maximum concentration of a drug in the body after dosing

L. T_{max}: the time it takes a drug or other substance to reach the maximum concentration C_{max}

M. PE: pomegranate extract

N. PJ: pomegranate juice

Introduction

1.1 Need for the Study

Pomegranate products, such as juice or extract, have been reported to have many beneficial effects including anti-oxidant [1,2], anti-inflammatory [3], and anti-proliferative properties [4]. Therefore, pomegranate may have the potential for the treatment of metabolic diseases (such as, obesity, diabetes, cardiovascular diseases) [5] or cancers [6,7].

Large quanlities of polyphenols (such as: ellagitannins (ETs), gallotannins, and anthocyanins) [1] and several phenolic acid (such as: gallic acid, chlorogenic acid, and coumaric acids) [8] have been identified in pomegranate products. Of these components, ETs were previously regarded as the major candidate responsible for health benefits [9]. However, there are some inconsistent results regarding the beneficial effects of pomegranate between *in vivo* and *in vitro* studies. One study showed that pomegranate juice supplementation failed to present benefits in patients with stable chronic obstructive pulmonary disease, the pathogenesis of which is closely related to oxidative stress [10]. According to another study, daily consumption of pomegranate juice did not alter prostate-specific antigen levels in male patients with advanced prostate cancer [11-13]. Studies focusing on CYP inhibition properties of pomegranate juice also reported inconsistent results *in vivo* from those *in vitro* [14]. These discrepancies might be explained by the low systemic availability of the major anti-oxidative components, such as ETs, in pomegranate. And the reported beneficial effects might be attributed to the metabolites found after absorption rather than the intact components of pomegranate [15].

1.2 The Process of Absorption and Metabolism after Pomegranate Consumption

ETs, the most likely candidates for health benefits *in vitro*, are large molecules and are poorly absorbed

[16]. After pomegranate consumption, ETs are hydrolyzed and converted into ellagic acid (EA). This hydrolysis is pH-dependent, with the optimal range at 7.0-7.3 [17]. Therefore, the release of free EA from ETs begins in the proximal small intestine. Regarding the bioavailability of EA, there are some controversies. Some studies showed that EA could not be detected in human plasma or urine after pomegranate juice consumption [10,16], while other studies reported that EA was detectable, but was quickly absorbed (T_{max} ~ 1h) and quickly eliminated ($t_{1/2E}$ ~ 0.71hr) [18,19]. EA is poorly absorbed in human stomach and small intestine. Its poor availability could be explained by its poor solubility, by its ionization and formation of insoluble complexes, or by its extensively binding to intestinal epithelium [15,18]. Absorbed EA first undergoes methyl conjugation by catechol O-methyl transferase (COMT) catalysis, and further conjugated with glucuronic acid forming dimethyl EA glucuronide (DMEAG) [15,17,20].

Urolithins are dibenzopyran-6-one derivatives with varying numbers of hydroxyl subgroups. The non-absorbed EA is metabolized by intestinal microbiota into urolithins, through the loss of one lactone and successive dehydroxylation [21]. This process requires microflorals, since no urolithins were found in germ-free animals [22]. The metabolism of EA begins in the jejunum. The first metabolite, urolithin M-5 (pentahydroxyl-urolithin), is formed after opening and decarboxylation of a lactone ring. Thereafter, tetrahydroxy-urolithins (urolithin D, urolithin M-6) are produced by removing one of the hydroxyl groups, followed by the formation of trihydroxy-urolithins (urolithin C, urolithin M-7), dihydroxy-urolithins (urolithin A and isourolithin A), and monohydroxy-urolithin (urolithin B) after the removal of a second, a third and a fourth hydroxyl group [21].

In the proximal intestine, urolithin D and urolithin C are produced, with significant concentrations in

the intestines, but only trace concentrations in plasma [23]. In the more distal parts, urolithin A and B are generated and urolithin B is the final product of ETs' microbial metabolism [23]. The absorption of urolithins increases in parallel with their lipophilicity [5]. The absorbed metabolites undergo glucuronide or sulfate conjugation. Urolithin A and urolithin B conjugates are the main metabolites which can be detected in plasma and urine, while the tetrahydroxy-urolithins and trihydroxy-urolithins are subject to enterohepatic circulation until their hydroxyl groups are removed, so that they can enter plasma and urine. This process is also responsible for the relatively slow elimination of urolithins by human body [5,15,18,21].

1.3 Major Metabolites of Pomegranate Consumption

In general, urolithin A-glucuronide and urolithin B-glucuronide are the two major products of under biotransformation. In our study, we choose 3 target analytes: ellagic acid (its bioavailability is in controversy), urolithin A, and urolithin B (2 main metabolites). By comparing incubation and non-incubation with β-deglucuronidase, free urolithin A, free urolithin B and their conjugates were both analyzed, with the objective of exploring their pharmacokinetic profiles in humans.

Materials and Methods

2.1 Standards and Reagents

Ellagic acid (CAS No. 476-66-4, 14668-50MG, ≥95.0%), chrysin (CAS No. 480-40-0, 95082-50MG, ≥98.0%) and Helix pomatia β-deglucuronidase (G-7017) were obtained from Sigma-Aldrich (St. Lousis, MO, USA). Urolithin A (CAS No. 1143-70-0, SC-475514, >98.0%) and Urolithin B (CAS No: 1139-83-9, SC-475547, >98.0%) were from Santa Cruz (Dallas, TX, USA). Organic solvents (LC/MS grade), including

methanol and acetonitrile were from Fisher Scientific (Waltham, MA, USA). Ultrapure water (LC/MS grade) was from Alfa Aesar (Ward Hill, MA, USA). All the solvents were used throughout our study. Filters (0.45μm) were obtained from ThermoFisher (Waltham, MA, USA).

2.2 LC-MS Instrumentation

Sample separation was achieved by using a LC-MS Agilent 1100 (Palo Alto, CA, USA) chromatography system, equipped with a degasser (G1379A, JP13209787), QuatPump (G1311A, DE23923540), auto-sampler (G1367A, DE12801210) and UV detector (G1316A, DE91612468). Ionization and detection were achieved by a API-3000 quadrupole mass spectrometer (MDS Sciex, Toronto, Canada) equipped with an electrospray ion (ESI) source, using Analyst as a control software. Multiple reaction monitoring (MRM) in negative mode was used to monitor precursor/ product ion transitions.

2.3 Stock Solutions

The stock solutions containing 20ng/μl of ellagic acid, 50ng/μl of urolithin-A, 50ng/μl of urolithin-B, 50ng/μl of chrysin (the internal standard) were prepared in methanol separately and stored at -20℃. Due to light sensitivity of ellagic acid, its stock solution was stored in an opaque container.

2.4 Calibration Curve Establishment

3 types of calibration curve were established: unextracted solution calibration curve, extraction method calibration curve, and matrix-matched calibration curve. These were quantitated by the analysis of different concentrations of EA, Uro-A, and Uro-B dissolved in clean mobile phase, spiked in human plasma followed by protein precipitation, or post-spiked in the identical matrix which undergoes the same procedure, respectively. Chrysin was used as an internal standard. Calibration curves were obtained by plotting peak area (y-axis) vs. concentration (x-axis) for each analyte, on the

basis of no significant variations in the peak area of internal standard. Regression equations and coefficient of determination (R^2) were obtained by linear regression analysis. Calibration lines were forced to cross the origin.

2.5 Matrix Effect Evaluation

To evaluate the matrix effect, the post-extraction spiked method was used[24,25], by comparing the peak area of an analyte in mobile phase versus the peak area of the analyte post-spiked into a blank matrix sample undergoing the sample preparation process. The equations to calculate matrix factor, matrix effect, recovery of extraction and process efficiency were as follows:

Matrix Factor (MF) = B/A

Matrix Effect (ME) = $B/A - 1$

Recovery of Extraction (RE) = C/B

Process Efficiency (PE) = C/A

(A) peak area of the analyte dissolved in mobile phase, (B) peak area of the analyte post-spiked into plasma after extraction, (C) peak area of the analyte pre-spiked into plasma before extraction.

MF = 1 indicates no matrix effect; MF > 1 indicates ion enhancement; MF < 1 indicates ion suppression [25].

2.6 Plasma Sampling Procedure

(1) Plasma treated without β-glucuronidase:

To test the concentrations of unconjugated analytes, 300μl plasma was spiked with internal standard (5ng/μl chrysin, 20ul), protein precipitated with 1000ul acetonitrile with 2% formic acid by shaking at 5 speed for 15min, and centrifuged at 14000rpm for 15min. After that, the liquid was filtered by a

0.45μm syringe filter and transferred into a clean tube. The solvent was completely evaporated at room temperature in a SpeedVac. Dried residuals were reconstituted in 120μl 50% acetonitrile, vortexed a few seconds, and centrifuged at 14000rpm for 10 min. The supernatant was transferred into an HPLC auto-sampling vial for LC-MS analysis.

(2) Plasma treated with β-glucuronidase [18]:

To test the total concentrations of analytes, including unconjugated and unconjugated forms, 300μl plasma was mixed with 50μl 0.2M KH_2PO_4 buffer and 30μl Helix pomatia β-glucuronidase (108,750units/ml). The pH of incubation mixture was verified during exploration of the incubation method: the final pH of incubation mixture was 4~5, based on the optimum pH of 4.2 for Helix pomatia β-glucuronidase[26]. The mixture was capped, vortexed and incubated at 37°C overnight avoiding light. Addition of 50μl 0.2M KH_2PO_4 buffer without Helix pomatia β-glucuronidase was adopted as the control. Thereafter, each sample was processed by protein precipitation described above.

Considering the optimum pH for Helix pomatia β-glucuronidase, KH_2PO_4 buffer was chosen to maintain the incubation mixture in an acidic environment. 0.2M KH_2PO_4 buffer was prepared by dissolving 13.6g KH_2PO_4 (0.2M *0.5L *136g/mol = 13.6g) into 0.5L distilled water. The PH was adjusted ~5 by adding 1M NaOH, and the solution was stored in 4°C until use.

2.7 Clinical Protocol

The samples were obtained from our previous study [14]. In general, 12 healthy volunteers (10 male, 2 female) were enrolled in our study. Each subject received the cotreatments for 3 different trials: Trial 1 (control), 250ml control beverage with low-polyphenol; Trial 2 (PJ trial), 250ml pomegranate juice; Trial 3 (PE trial), 1g capsule of pomegranate extract. The sequence of the 3 trials was determined by

computer randomization. The trials were separated by at least 1 week. Within each trial, the treatments were administered twice: one at 4~6pm, the other one at 7:30am next morning. After these 2 administrations, venous blood samples were drawn for plasma collection at various time points up to 12.5 hours after dosage.

The total polyphenol content of the pomegranate juice was 3.2~3.3mg/ml, and that of pomegranate extract was 689mg/capsule, while for the control beverage, the total polyphenol content was 0.11~0.12mg/ml. In sum, a single-dose consumption of 250ml pomegranate juice provided ~800mg polyphenol content intake, and a single-dose consumption of 1g capsule pomegranate extract provided 689mg of polyphenol.

Results

3.1 General Characteristics of Compounds

The data on compound names, molecular formula, and structures are shown in Table 1.

Table 1: General characteristics of the analytes

Compound	Molecular formula	structure	pka
Ellagic acid	$C_{14}H_6O_8$	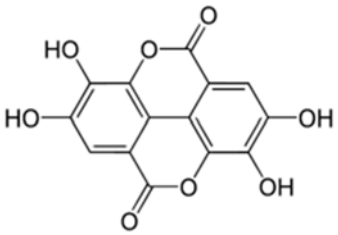	5.54
Uro-A	$C_{13}H_8O_4$	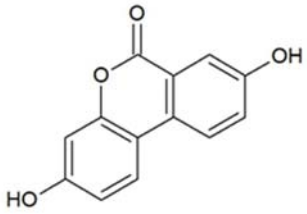	7.21
Uro-B	$C_{13}H_8O_3$	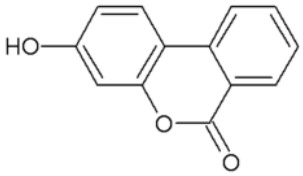	N/A
Chrysin (Internal standard)	$C_{15}H_{10}O_4$	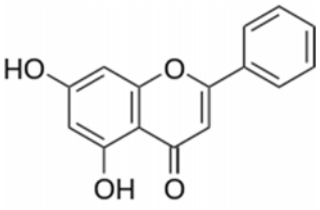	6.87

3.2 Method Development

Method development includes two parts: LC-MS method development and sample extraction method development.

3.2.1 LC-MS method development

(1) LC method development

LC separations were carried out on a reverse phase Poroshell 120 EC-C18 column (3 × 100 mm, 2.7um; Agilent) using water: formic acid (99.9: 0.1, v/v; phase A) and acetonitrile: formic acid (99.9: 0.1, v/v; phase B) as the mobile phases at a flow rate of 0.4mL/min. The UV detection wavelength was set at 254nm. A 5μl sample solution was injected into the column. The gradient program was as follows:

Total Time (min)	A (%)	B (%)
0.00	95.0	5.0
5.00	80.0	20.0
9.00	50.0	50.0
12.00	10.0	90.0
13.00	95.0	5.0
18.00	95.0	5.0

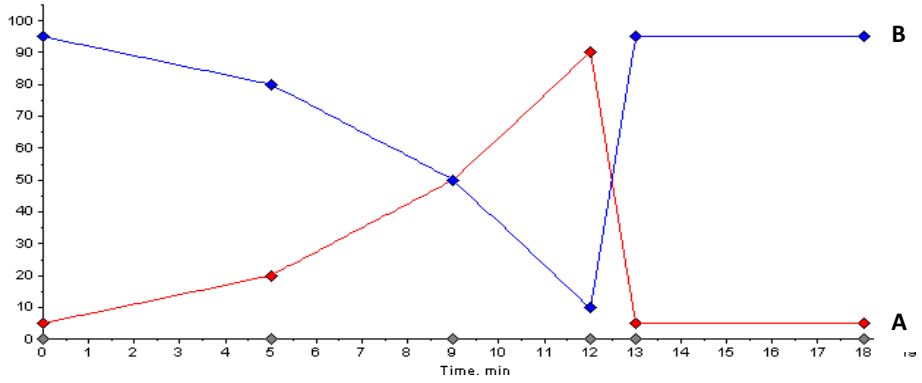

(2) MS method development

a. Compound-dependent parameter optimization -- Infusion Tuning

Both negative ion mode and positive ion mode were evaluated. The MS instrument response for Uro-A and Uro-B was higher with the positive ion mode. However, considering that ellagic acid cannot be detected under positive ion mode, the negative ion mode was finally used for the analysis of all the compounds simutaneously. Optimization of the quantitation process for an MS/MS analysis was performed by MS with an infusion device. Under the tuning mode, precursor ion, product ion and compound-dependent parameters, declustering potential (DP), focusing potential (FP), collision energy

(CE) and collision cell exit potential (CXP), were optimized for each analyte. In order to achieve maximum instrument response, EA was identified by 300.927→145.000, Uro-A by 226.977→197.900, Uro-B by 210.915→166.600, chrysin by 252.935→62.900. The optimized values of DP, FP, CE and CXP for each analyte were as follows (Table 2).

Table 2: Compound-dependent parameters optimization -- Infusion Tuning

	m/z	MS/MS	DP	FP	CXP	CE
EA	300.927	41.100; 117.000; **145.000**; 172.900; 184.800; 200.700; 228.900; 244.900	-96	-270	-23	-56
Uro-A	226.977	41.100; 129.000; 153.600; 154.000; 170.700; 181.900; 183.000; **197.900**	-61	-250	-35	-44
Uro-B	210.915	168.788; 64.900; 116.800; 137.800; 138.800; 140.800; **166.600**; 169.000	-66	-240	-29	-34
Chrysin	252.935	41.000; **62.900**; 64.900; 106.800; 107.000; 119.000; 142.900; 144.900	-61	-210	-5	-56

The most intense product ion is printed in boldface.

(2) Source-dependent parameters optimization -- Flow Injection Analysis (FIA)

LC-MS interface parameters are critical for the sensitivity of the LC-MS instrument. Based on the available compound-dependent parameters from infusion tuning, FIA was performed to optimize the source-dependent parameters.

The LC conditions used for FIA tuning were as follows: mobile phase of 60% acetonitrile with 0.1% formic acid and a flow rate of 0.4mL/min. Turbo ionspray gas (Gas2) flow was 7L/min. To obtain reliable results, concentrations of the 3 analytes and internal standard in the sample for injection were set as follows: EA=100ng/μl, Uro-A=50ng/μl, Uro-B=50ng/μl, chrysin=25ng/μl, to ensure signal-to-noise ratio > 20:1. 4 replicate injections for each step value. The instrument response of each analyte for each parameter at each step value was shown in Table 3. In order to maximize instrument sensitivity

and minimize background noise, the final value of source and gas parameters were set as nebulizer gas of 12, curtain gas of 8, collision gas of 7, ionspray voltage of -2000V, temperature of 450℃. The chromatograms of the analytes by the established LC-MS method were shown in Figure 1.

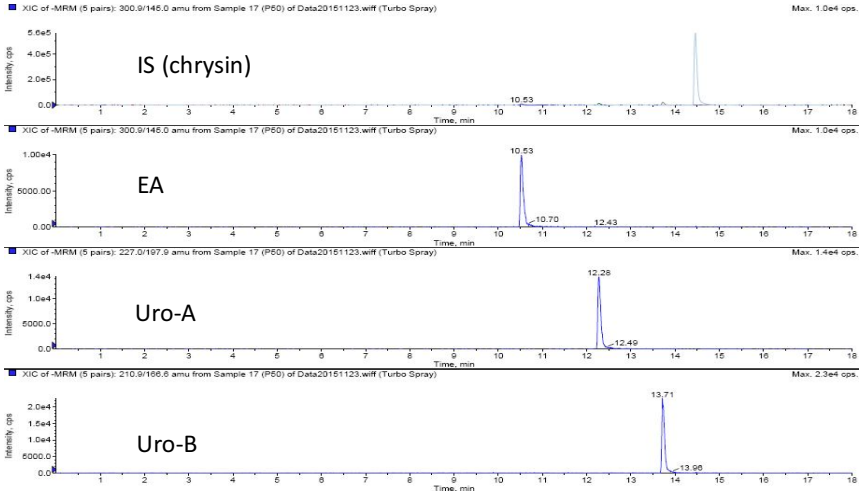

Figure 1: LC-MS extracted ion chromatograms showing the 3 target analytes dissolved in clean solvent.

Table 3: Source-dependent parameters optimization -- FIA tuning

Step value	EA	Uro-A	Uro-B	chrysin
Nebulizer (psig)				
8	2460±387.3	1957±329.5	4580±661.3	9443±938.5
10	2427±107.2	2058±164.6	3620±84.5	9213±340.8
12	2342±204.5	1975±50.0	3463±59.1	9430±566.0
14	2782±141.5	2093±229.1	3415±177.1	9570±483.5
optimal	14	14	8	14
final	12			
Curtain Gas (psig)				
8	2632±138.4	2227±259.8	4348±295.8	11253±743.9
10	1877±254.9	1618±86.9	2895±14.2	7678±453.8
12	1515±142.5	1378±66.5	2395±98.8	6245±598.2
14	950±123.3	960±63.8	1663±143.8	3973±337.5
optimal	8	8	8	8
final	8			
Collision Gas (psig)				
4	1190±111.1	1235±164.2	1993±196.2	6140±392.2
5	1538±78.0	1648±140.8	2993±307.4	7685±359.3
6	1738±131.2	1963±201.1	3063±158.0	8270±396.7
7	1668±184.5	1958±139.4	3460±306.4	8273±577.8
optimal	6	6	7	7
final	7			
IonSpray Voltage (V)				
-2000	1475±59.2	1798±130.2	3640±135.9	8735±771.6
-2500	1260±59.4	2008±175.6	3043±165.2	6813±331.8
-3000	1165±92.6	1860±253.9	2870±68.8	6050±224.9
-3500	1060±69.8	1883±128.9	2828±123.9	5805±391.8
-4000	975±95.7	1790±51.0	2903±144.5	5515±433.1
optimal	-2000	-2500	-2000	-2000
final	-2000			
Temperature (℃)				
250	933±113.2	1850±114.3	3158±90.7	6865±260.3
300	798±62.9	1988±156.3	3595±148.0	8003±527.4
350	965±148.0	2185±75.1	3988±270.8	10278±534.2
400	1000±86.8	2063±175.9	4508±447.9	11090±931.5
450	980±66.8	2470±137.4	6015±419.3	15423±1230.3
optimal	400	450	450	450
final	450			

3.2.2 Sample extraction method development

For plasma sample preparation, protein precipitation and liquid-liquid extraction were both tried during method development. For protein precipitation agents, we compared methanol with acetonitrile. Acetonitrile is better than methanol for sample purification, but only acetonitrile failed to extract EA from plasma (recovery~0). Since EA could only be efficiently extracted in an acidic environment [18,27,28], we used acetonitrile with 2% formic acid to ensure an acceptable recovery for each analyte. Several commonly used organic solvents were also tried for liquid-liquid extraction, such as ethyl ether, isobutanol, and toluene. However, the appropriate organic which can efficiently extract 4 compounds from plasma simultaneously could not be identified. Therefore, although protein precipitation is not an ideal choice for obtaining a clean sample, we used protein precipitation using acetonitrile with 2% formic acid for sample preparation. In a balance of the limited available plasma volume and the necessary instrument sensitivity, we finally used 300µl plasma reconstituted in 120µl 50% acetonitrile after protein precipitation for LC-MS analysis.

3.3 Method Validation

3.3.1 LC-MS stability

Instrument stability was evaluated by 6 replicate injections for one sample (EA=20ng/ml, Uro-A=10ng/ml, Uro-B=10ng/ml) after method development. The constant variations (CV) of each analyte peak area, internal standard peak area, and analyte versus internal standard peak area ratio were all less than 5%, which showed the established LC-MS method was stable (Table 4).

Table 4: LC-MS stability (6 replicate injections)

Analyte Peak Name	Analyte Peak Area (counts)	IS Peak Area (counts)	AREA RATIO
EA	7150	1660000	0.004307
	7720	1630000	0.004736
	7490	1640000	0.004567
	7380	1670000	0.004419
	7870	1630000	0.004828
	7190	1600000	0.004494
Mean	7466.7	1638333.3	0.0045585
SD	287.0	24832.8	0.0001955
CV (%)	4	2	4
Uro-A	22700	1660000	0.013675
	21300	1630000	0.013067
	21700	1640000	0.013232
	21500	1670000	0.012874
	22200	1630000	0.013620
	21500	1600000	0.013438
Mean	21816.7	1638333.3	0.0133177
SD	530.7	24832.8	0.0003164
CV (%)	2	2	2
Uro-B	51700	1660000	0.031145
	54100	1630000	0.033190
	52000	1640000	0.031707
	51400	1670000	0.030778
	49600	1630000	0.030429
	51500	1600000	0.032188
Mean	51716.7	1638333.3	0.0315728
SD	1441.4	24832.8	0.0010134
CV (%)	3	2	3

3.3.2 Calibration curve

Analyte standards dissolved in neat solvent showed good linearity for EA, Uro-A and Uro-B (R^2>0.99). Due to limited human plasma, we initially used bovine serum to develop extraction method and to test linearity of the samples undergoing protein precipitation, which also showed good linearity (R^2>0.995) (Table 5).

Table 5: Linearity

	Calibration Curve		Conc. Range
	Equation	R^2	(ng/mL)
Pure			
EA	y = 617.98x	0.9964	2~200
Uro-A	y = 1272.9x	0.9902	1~500
Uro-B	y = 2197.2x	0.9939	1~100
Extracted			
EA	y = 741.4x	0.9997	2~200
Uro-A	y = 1007x	0.9965	1~500
Uro-B	y = 1192.3x	0.9996	1~100

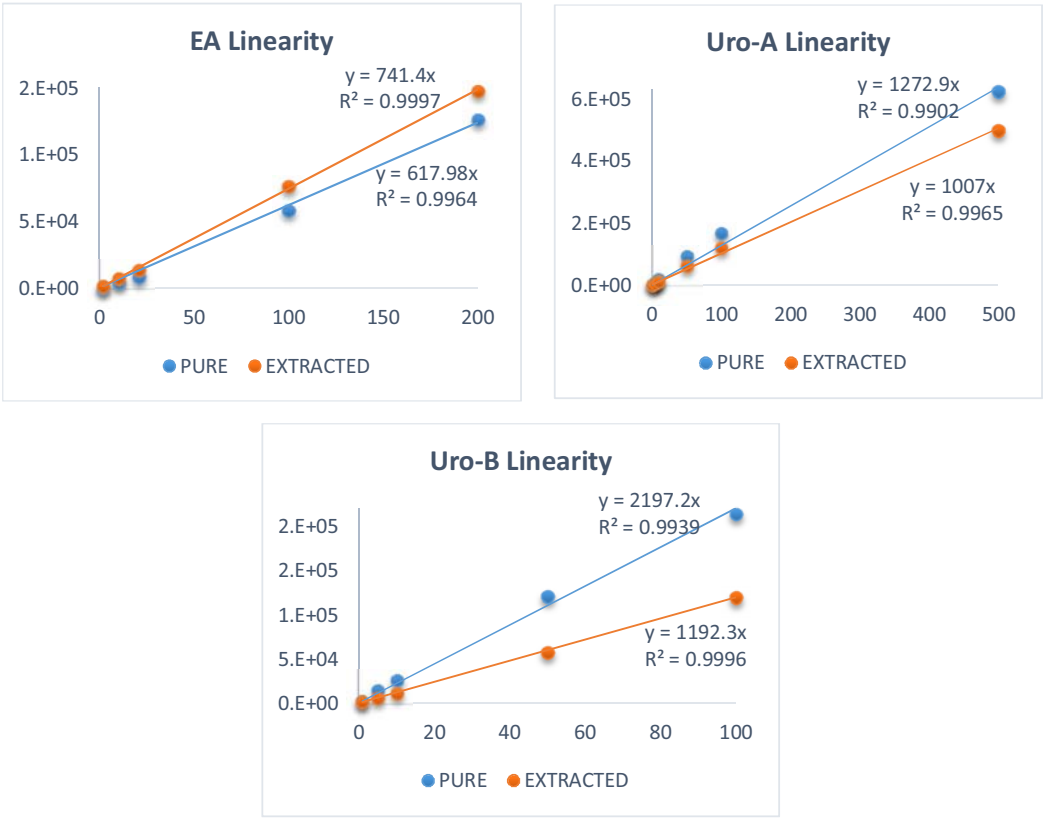

Figure 2: Linearity graph of the analytes (pure vs. extracted)

3.3.3 Matrix Effect

However, it was unexpected that the peak areas of EA in pre-spiked (extracted) samples were much

higher than those dissolved in mobile phase at the same concentration. The peak area ratio of pure samples versus extracted sample ranged from 1.17 ~ 2.88. This phenomenon cannot be simply explained as an error, since the enhancement of peak area was too large. It became more obvious in a lower concentration (Table 6).

Table 6: Peak area of EA in pure samples vs. in extracted samples

Conc. of EA	Peak Area in Pure Samples	Peak Area in Extracted Samples	Peak Area Ratio of E/P
2	540	1555	2.88
10	4220	7350	1.75
20	8120	13600	1.67
100	58050	75950	1.31
200	126000	147500	1.17

After we consulted Dr. Chen at Tufts Nutrition Center and reviewed relevant articles, the matrix effect was highly suspected as the potential reason for this phenomenon. Therefore, we evaluated matrix effect in both bovine serum and human plasma (Table 7). The concentrations we used were as follows: EA=20ng/ml, Uro-A=10ng/ml, Uro-B=10ng/ml.

Table 7: Matrix effect evaluation (human plasma vs. bovine serum, without filters)

Compounds		Volunteer No.		B.S.
		3	10	
EA	ME (%)	-94	-76	80
	RE (%)	104	72	82
	PE (%)	7	17	148
Uro-A	ME (%)	-87	-65	-17
	RE (%)	76	91	99
	PE (%)	10	32	82
Uro-B	ME (%)	-11	-31	-19
	RE (%)	99	108	93
	PE (%)	88	74	111

Abbreviations are defined in section 2.5.

Table 7 showed matrix effects were very different between human plasma and bovine serum. For EA,

there was ion enhancement in bovine serum, but ion suppression in human plasma. For Uro-A and Uro-B, bovine serum and human plasma both showed ion suppression.

Different methods were evaluated to eliminate or inhibit matrix effect. For LC method, we tried lower injection volumes, lower flow rates, splitting flow, and different gradients with longer durations, which all failed to effectively inhibit matrix effect but significantly impaired method sensitivity. For the MS method, we tried to adjust source and gas parameters. However, this did not work well either. For the extraction method, we tried protein precipitation by methanol and acetonitrile with 2% formic acid. Acetonitrile was better than methanol. We did not determine the appropriate organic solvent for liquid-liquid extraction, so we still used protein precipitation with 2% formic acid acetonitrile. Some articles also mention using filters before injection into LC-MS [16,28], and we also tried filters with 0.45μm pore size. Matrix effect with or without filters was -0.14 vs. -0.65, -0.38 vs. -0.50, and -0.21 vs. -0.41 for EA, Uro-A and Uro-B respectively, which showed filters could relieve matrix effects to some extent, but they cannot completely eliminate matrix effects. Therefore, filters were used in the following experiments (Table 8).

Table 8: Matrix effect evaluation (with or without filters)

Compounds		Without filters	With filters
EA	ME (%)	-65	-14
	RE (%)	90	120
	PE (%)	31	103
Uro-A	ME (%)	-50	-38
	RE (%)	91	113
	PE (%)	45	70
Uro-B	ME (%)	-41	-21
	RE (%)	107	105
	PE (%)	63	83

After that, we evaluated the inter-individual variability in matrix effect, since if there is an heterogeneity, it is not valid to calculate the concentration of an analyte using the calibration curve generated from the plasma of a different individual. According to Matuszewski *et al* [29], at least 5 matrices should be used to assess matrix effect. Therefore, we selected the plasma from 5 different subjects to evaluate matrix effect separately. Results showed CVs of matrix effects for EA, Uro-A and Uro-B were 43%, 24% and 44% respectively, which means matrix effect varied among different human individuals (Table 9).

Table 9: Matrix effect evaluation among 5 different individuals

Compounds		**Volunteer no.**					**CV (%)**
		4	9	1	11	8	
EA	**ME (%)**	-45	-65	-14	-59	-59	43
	RE (%)	108	121	120	103	76	17
	PE (%)	60	79	103	42	31	46
Uro-A	**ME (%)**	-58	-56	-38	-36	-37	24
	RE (%)	93	106	113	94	97	9
	PE (%)	40	47	70	60	62	22
Uro-B	**ME (%)**	-55	-24	-21	-25	-43	44
	RE (%)	93	96	105	107	106	6
	PE (%)	41	73	83	81	60	26

Because the matrix effect could not be completely eliminated and varied among different individuals, we finally settled on matrix-matched calibration[30] for analytical quantification. As long as the sensitivity allowed, we would use matrix-matched calibration for the further analysis.

3.4 Pharmacokinetic Profiles of 3 Analytes in Humans

3.4.1 A pilot study to evaluate matrix-matched calibration

In order to test the feasibility of matrix-matched calibration, we selected 1 subject (volunteer No.11) and used the plasma sample in control trial to establish 3 types of calibration curves, and tested free

and total concentrations of these metabolites in PE and PJ trials respectively. Due to the limited amount of plasma, we only adopted 3 different concentration to generate the calibration curves (EA concentrations: 10ng/ml, 100ng/ml, 200ng/ml; Uro-A & Uro-B: 5ng/ml, 50ng/ml, 100ng/ml) (Figure 3). The sensitivity for EA, Uro-A and Uro-B was acceptable. In the control group, none of these 3 analytes, neither free nor total, were detected. At 4.5 hour after administration (Table 10), total EA of 32ng/ml and total Uro-A of 83ng/ml were detected in the plasma from PJ trial, after incubation with β-glucuronidase. Total Uro-A of 19ng/ml was detected in the plasma from PE trial, whereas EA was non-detectable. Most detected EA was unconjugated, while all detected Uro-A was conjugated. Uro-B, no matter unconjugated or conjugated, cannot be tested at the time point of 4.5 hour. At 8.5 hour after beverage or extract consumption (Table 11), EA was no longer detectable. All detected Uro-A was conjugated, with 112ng/ml in PJ trial and 23ng/ml in PE trial. Trace concentrations of conjugated Uro-B, 3ng/ml, was detected in both PJ and PE trials.

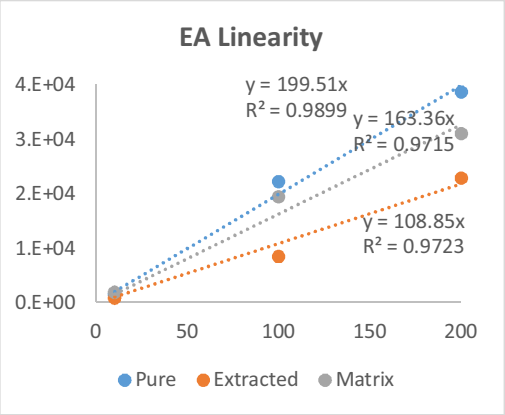

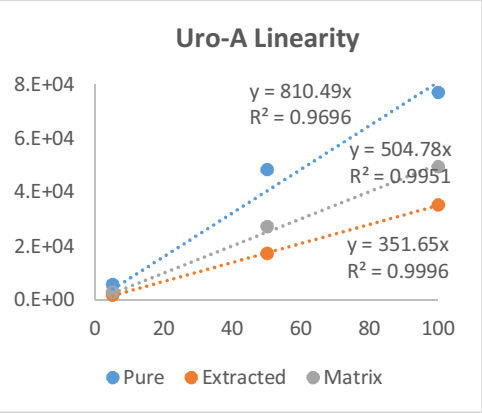

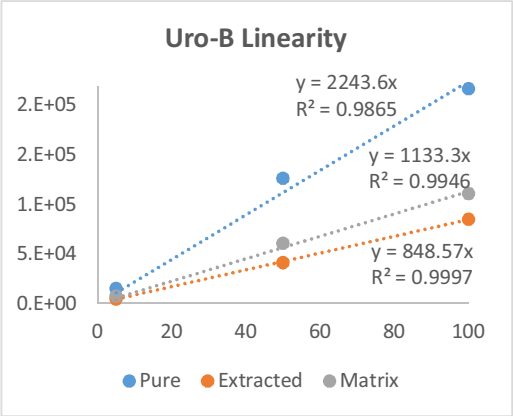

Figure 3: Linearity of matrix-matched calibration

Table 10: Plasma concentrations of the analytes at 4.5 hour after administration (ng/ml)

Trials	EA		Uro-A		Uro-B	
	Free	Total	Free	Total	Free	Total
Pome Juice	23	32	-	83	-	-
Pome Extract	-	-	-	19	-	-
control	-	-	-	-	-	-

Table 11: Plasma concentrations of the analytes at 8.5 hours after administration (ng/ml)

Trials	EA		Uro-A		Uro-B	
	Free	Total	Free	Total	Free	Total
Pome Juice	-	-	-	112	-	3
Pome Extract	-	-	-	23	-	3
control	-	-	-	-	-	-

3.4.2 Pharmacokinetic profiles of 3 analytes in one subject

After cleaning of the interior of the MS and retuning the analytes, we selected another subject (volunteer No. 3), calculated the calibration curves, and tested the concentrations of the analytes at all the time points.

Linearity of each calibration curve for every target analyte was good (R^2>0.99) (Figure 4). PE, RE and ME for each analyte were similar at different concentrations (Table 12), except for the low

concentration of EA. T_{max} for EA occured within 1h after pomegranate product administration. Both PE and PJ trials showed fast absoption and quickly elimination of EA. EA nearly could not be detected after 6 hrs. Incubation with β-glucuronidase did not make a significant difference in the plasma concentration of EA. However, PE and PJ trials showed different metabolic profiles of EA (Figure 5, Table 13). Administration of PE showed a higher peak of concentration-vs-time curve and a faster elimination when compared with PJ, while the areas under the curve (AUC) were very similar with each other.

For the metabolic profile of Uro-A (Figure 6), unconjugated Uro-A could not be detected in either PE or PJ trial. After deglucuronidation, Uro-A glur was still undetectable in PE trial, while the concentration of Uro-A glur was significantly enhanced after the 2nd dose of PJ. T_{max} of Uro-A glur would occur after 12 hours after administration. Neither free Uro-B nor conjugated Uro-B were detected in PE or PJ trial in this subject.

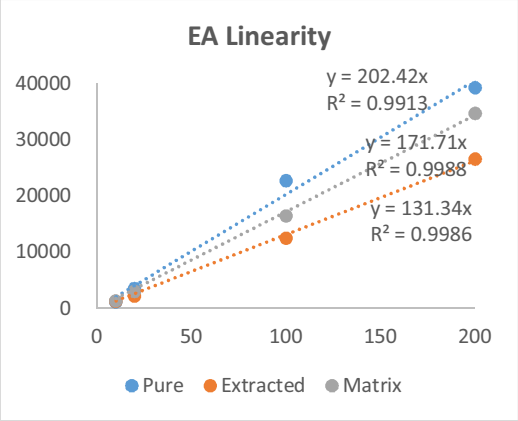

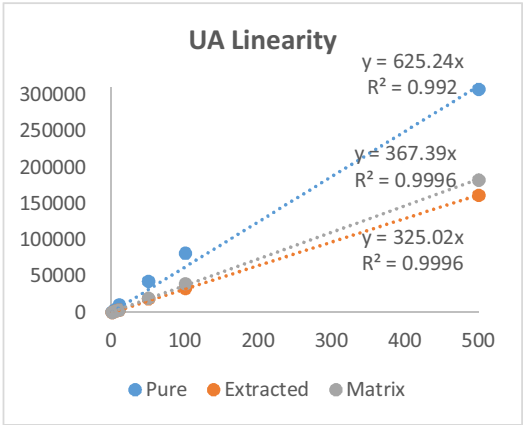

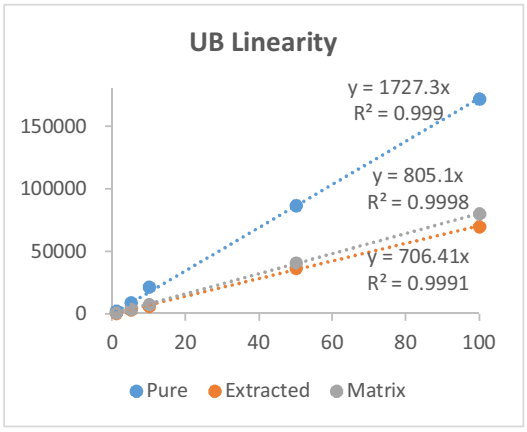

Figure 4: Linearity of matrix-matched calibration

Table 12: Process efficiency, recovery of extraction, matrix effect at different time points for 3 analytes

conc.	Uro-A (%)			conc.	Uro-B			conc.	EA		
(ng/ml)	PE	ME	RE	(ng/ml)	PE	ME	RE	(ng/ml)	PE	ME	RE
1	49	-55	107	1	37	-54	81	10	109	26	87
5	43	-58	103	5	39	-58	93	20	64	-13	73
10	32	-66	92	10	29	-65	84	100	55	-28	76
50	44	-55	96	50	42	-53	90	200	68	-12	77
100	41	-51	85	100	41	-53	87				
500	53	-40	89								
mean	42	-57	97		38	-57	87		74	-7	78
SD	7	8	8		5	5	5		24	23	6

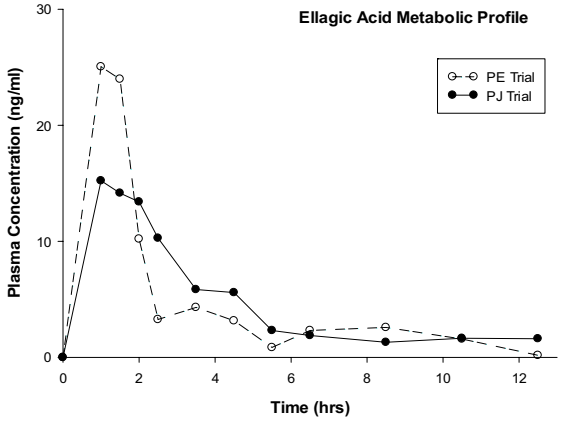

Figure 5: Ellagic acid metabolic profile

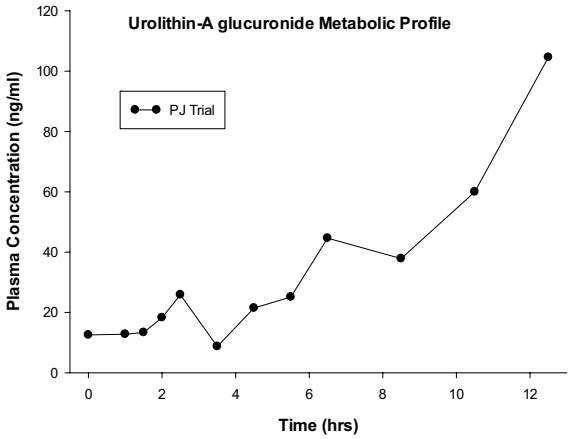

Figure 6: Uro-A glucuronide metabolic profile

Table 13: Pharmacokinetic parameters for free EA

	PE Trial	PJ Trial
C_{max}, ng/ml	25.0	15.2
T_{max}, h	~1h	~1h
AUC, (ng*h)/ml	58.597	56.986

Discussion and Future Directions

4.1 Analyte Optimization

Optimization was performed to maximize the sensitivity of LC-MS method. If sensitivity allows, optimization is not necessary for all the experiments. However, in our study, the default values of parameters failed to provide good sensitivity to detect EA, which even if the concentration was around 50ng/ml. Therefore, optimization was needed to improve the sensitivity of the analytes, esp. for EA. Infusion tuning and introducing the standard solution into MS directly by a syringe pump, was used to optimize the molecular weight of precursor and product ions, and also the compound-dependent parameters (DP, FP, CE and CXP). This method is fast and convenient, but the lack of LC conditions, such as flow rate and mobile phase, fails to match the real conditions[31]. To overcome these disadvantages

and to further optimize the source-dependent parameters, FIA tuning was also performed. To achieve a reliable result, the solution with a sufficient concentration ensuring signal-to-noise ratio >20:1 was injected by HPLC auto-sampling device. To mimic the actual LC conditions, a flow rate of 400µl/min and the mobile phase of 60% acetonitrile was adopted.

Nebulizer gas (NEB) is responsible for the nebulization for sample solution going through the sprayer needle, and is a determinant of signal stability and sensitivity [31]. In our results, the highest sensitivity of EA, Uro-A and chrysin was reached at NEB of 14. However, NEB of 14 significantly increased the background noise and resulted in an unacceptable high CV (16% in 6 replicates). On balance, NEB of 12 was finally set.

Curtain gas (CUR) prevents the contamination and ensures a stable clean environment during the process of introducing sample ions. CUR should be maintained as high as possible without significantly impairing signal sensitivity [32]. In our study, the best sensitivity of all analytes was achieved at the CUR starting value of 8. As CUR value increased, instrument response of all the analytes significantly decreased. Therefore, CUR of 8 was the optimal value we chose finally.

Ionspray voltage is the potential, maintained between capillary entrance and the sprayer needle, to bring about the electrospraying process [31]. The negative ion mode usually uses a lower voltage. Excessively high voltage leads to unstable spray configuration and may cause damage to the instrument [33]. In our work, a voltage of -2000 was optimal for EA, Uro-B and chrysin. Even if it was not the optimal value for Uro-A, Uro-A sensitivity at a voltage of -2000 was sufficient for analysis. Therefore, -2000 was set as the optimal value.

Collision-activated dissociation gas (CAD) is responsible for the fragmentation of product ions. The

degree of ion fragmentation increases as the mass of the collision gas increases [34]. In our study, the highest instrument response for each analyte was obtained at CAD of 7, which was set as the final value. .

Temperature (TEM) is required to ensure the complete evaporation of LC solvent for the generation of ions. TEM is dependent on 2 factors: LC flow rate and organic content of mobile phase. The optimal TEM is positively correlated with the LC flow rates, while negatively correlated with the organic proportion in the mobile phase. Sufficient heat is needed for the solvent evaporation, while too much heat will cause unwanted decomposition and excessive background noise [33]. We found that the optimal value for Uro-A, Uro-B and chrysin was 450, while the highest instrument response for EA was reached at TEM of 400. However, the differences of EA signal between TEM of 400 and 450 were not statistically significant. So finally TEM of 450 was adopted as the optimal value.

4.2 Range Estimation of Calibration Curve

Determining the range of calibration curve is a critical step, since it should cover the potential maximum concentration of analyte in real plasma samples.

For EA, there are different studies focusing EA bioavailability, with variable results. The lack of detectable EA in human plasma after pomegranate consumption was reported in some studies [28], while in other studies plasma EA concentrations were reported to be detectable, with C_{max} ranging from tens to hundreds of ng/ml [18,19,27,35,36], based on different composition of intake and different clinical protocols. According to Seeram *et al* [27], after the consumption of 180ml pomegranate juice (with 25mg EA and 318mg ETs), C_{max} of EA in one healthy subject was ~31.9ng/ml. In their subsequent study, expanding the study subjects to 18 healthy individuals under the same

treatment, C_{max} of EA was 0.06 ± 0.01 µmol/L (18.12 ± 3.02 ng/ml) [18]. In another study, of 11 healthy subjects after administration of 800mg pomegranate extract (containing 330.4mg major ellagitannins punicalagins and 21.6mg EA), C_{max} for EA was determined as 33.8 ± 12.7 ng/ml [35]. Additionally, the mean value of C_{max} for EA in another study, after 3 treatments with 857mg, 776mg, and 755mg polyphenols, was 0.06, 0.04, and 0.02µmol/L (18.12ng/ml, 12.08ng/ml, 6.04ng/ml) in 16 healthy volunteers, respectively [19].

In our study, the composition of pomegranate juice/ extract (800mg polyphenols contained in single dose of juice and 689mg polyphenols contained in single dose of extract) was similar to those in these studies mentioned above. Although our study used 2-dose administration, the interval between the 2 doses was more than 12hrs. Therefore, a large amount of absorbed EA from the 1st dose was eliminated before the 2nd dose was administrated. As such, C_{max} of EA in our study should not be too much different from the reported ones. Therefore, the upper limit of 200ng/ml was set as the range for EA calibration.

However, C_{max} of ~200ng/ml EA was also reported in one study [36], which used direct administration of 40mg EA capsule. In fact, the EA content in pomegranate juice is usually less than 20mg/L in most cases [5], which means the consumption of 200mg pomegranate juice would provide ~4mg EA. In addition, the formulation of ETs with EA might also impair the absorption of EA, since ETs are not absorbable by human gastrointestinal tract [16]. These factors might explain the inconsistent results in this study from those in the studies mentioned above. Therefore, C_{max} of EA in our study is not likely to be that high.

Pharmacokinetic studies of Uro-A and Uro-B are fewer than those of EA, especially for Uro-B. There is

a study focusing on the metabolic profile of urolithins in colorectal cancer patients, with pomegranate extracts administrated 2/day for more than 10 days [28]. Since urolithins can persist for more than 48 hrs [18,19], there could be accumulation from several doses, and the concentration of Uro-A and Uro-B would be too high to be taken as a reference. In a study with a single-dose of ~400mg polyphenols, the total Uro-A and Uro-B concentrations (after treatment with glucuronidase and sulfatase enzymes) in plasma were quantitated at two different time points after administration: 0.04μmol/L (9.12ng/ml) and 0.02μmol/L (4.24ng/ml) at 0.5h; 0.11μmol/L (25.08ng/ml) and 0.05μmol/L (10.6ng/ml) at 6h, respectively [18]. In a study with single doses of ~800mg polyphenols, most of Uro-A glucuronide fell in the range of 0~500ng/ml within 12hrs [19]. Therefore, we established Uro-A range of 0~500ng/ml and Uro-B range of 0~100ng/ml provisionally.

4.3 Matrix Effect

A matrix effect can be responsible for different responses of an analyte in a biological matrix compared to a pure solvent[37]. The co-eluting components in matrix influence the ionization of the target analyte, producing either ion suppression or ion enhancement [38].

The matrix effect occurs at the LC-MS interface where the solvent is evaporated and the analyte is ionized. Of all the ion sources, ESI source is the most susceptible source to matrix effects. In an ESI source, the analyte firstly needs to obtain charge in the solvent, and then transitions to the gas phase with the charge [39,40]. Since MS can only detect and analyze charged irons (positive or negative) rather than neutral molecules, any factor which has the potential to interfere with the process of solvent evaporation or analyte ionization is likely to generate a matrix effect [39,40]. The endogenous matrix components, such as phospholipids and fatty acids, can inhibit the ionization of the analyte by

competing for the charge on the droplet surface. The presence of impurities can also prevent the analyte's transition into the gas phase through an increase in the viscosity and surface tension of the droplets [41]. Besides, exogenous compounds, such as the anticoagulant Li-heparin, can also cause a matrix effect [42].

There are two commonly used method to evaluate matrix effects: (1) the post-column infusion method (a qualitative assessment), (2) the post-extraction spike method (a quantitative assessment) [38]. In our study, we chose the latter one. Results showed that all the 3 target analytes had matrix effects in human plasma and matrix effects varied in different individuals.

How to reduce matrix effect? In method development, there are 3 important parts: sample preparation, separation (LC), and detection (MS) [43]. Therefore, the methods for decreasing or eliminating matrix effects also involve in these 3 areas.

Usually, a matrix effect is caused by the insufficient sample purification. Therefore, developing a proper sample extraction method is of primary importance [41]. Protein precipitation is the simplest and fastest way, but it is also the most likely way to induce matrix effect[24]. Although protein precipitation can remove most of the proteins (>90%) at a 2:1 ratio of precipitant to plasma [44], it fails to efficiently get rid of other endogenous components, such as phospholipids, which have been regarded as the major sources for the development of matrix effects. It was showed that acetonitrile can remove more phospholipids compared with methanol. However, significant matrix effects (67-77% ion suppression) still existed in the prepared samples even with acetonitrile [38]. In our study, we used acetonitrile with 2% formic acid for protein precipitation. Without filters, matrix effects were very significant for 3 analytes, esp. for ellagic acid.

Liquid-liquid extraction and solid-phase extraction are better alternative choices for sample preparation and clean-up. However, due to different chemical properties of EA, Uro-A, and Uro-B, we did not find a single appropriate organic solvent to sufficiently extract all the 3 target analytes simultaneously. In previous studies, protein precipitation in an acidic environment was adopted in most cases to collect EA or urolithins from human plasma [16,18,27,28,35]. We also used filters with 0.45µm pore size to try to remove some interfering materials. It was shown that these filters could ameliorate ion suppression in human plasma to some extent, but they could not eliminate all of these effects.

Optimization of LC method can also help to reduce matrix effects. PH value and mobile phase gradient are both the factors which can affect the matrix effect. Because the least hydrophobic phospholipids, usually eluted in the earliest phase, are independent of pH; more hydrophobic di-alkyl phospholipids need a longer organic hold and a higher pH to be completely eluted [38]. Manipulating the mobile phase pH can change the retention time of the target analytes and separate them from the chromatographic regions more likely containing phospholipids and susceptibility to ion suppression [38]. Besides, smaller injection volume or sample dilution may also decrease matrix effects, since these strategies also decrease the contaminant concentration in the interface. However, they will also significantly impair the sensitivity of the method [45]. In our study, due to the relatively low sensitivity of EA (LOQ ~10ng/mL in human plasma), these 2 solutions were not practical in our cases.

For MS conditions, APCI interface is more resistant to matrix effects [46]. However, it was not practical for us to change into an alternative ion source. Lower flow rates or flow splitting may also be helpful in relieving matrix effects. They result in the smaller charged droplets, less droplet fragmentation events, and less solvent evaporation during ion transition in the gas phase, which may all lead to a reduction

in the impurity concentration[24]. However, lower flow rates will also cause longer retention times and flow splitting will result in partial loss of the analytes which cannot enter into the MS detector and analyzer. So both of them will reduce sensitivity. Our results showed that lower flow rates and flow splitting did not significantly suppress matrix effects, and obviously decreased the sensitivity. Therefore, they were also not applicable in our study. In addition, negative or positive mode responsed differently for matrix effects. The negative mode was reported to be more specific and resistant to ion suppression[24,45]. However, choosing which kind of mode should be dependent on the ionization property of the target analyte. In our study, we selected the negative mode initially, so there was nothing to change in this respect.

Matrix effects are very complex and difficult to completely eliminate. If they are still unavoidable in analyses of real samples, like our study, there are still two method to compensate for matrix effects.

The first one is to the use of an appropriate internal standard, ideally the target analyte isotopes, which have the similar properties of instrument response. In another words, an analyte and its internal standard could present the changes of signal in a biology matrix to the same degree, so that the calibration curve based on the signal ratio of analyte versus internal standard will not be changed. Therefore, a proper internal standard could be used to correct a moderate no-additive matrix effect, as long as the sensitivity allows [30]. However, the isotopes are very expensive and difficult to locate. We only found a vendor for urolithin-B isotope, while ellagic acid and urolithin-A isotope are still not available.

Another solution is to adopt a matrix-matched calibration, which is the calibration curve prepared in an identical matrix free from target analyte [30]. We had tested 6 human plamsa samples in control

group, and no target analytes were detected. Therefore, we decided to use matrix-matched calibration for further analysis.

4.4 Pharmacokinetic Profiles

In general, the available results in our study were in agreement with the published results and our expectations:

(1) For EA, free EA was detected in our study. It was previously reported that EA-glucuronide was not detected in plasma, urine and colon tissues samples [28], which is also similar to our results. In addition, pharmacokinetic parameters for EA (such as, T_{max}, C_{max}, and AUC) were in accordance with the reported values[18,35]. (2) For Uro-A, all detected Uro-A in 2 subjects was conjugated, and the peak of Uro-A concentration was likely to occur 12hrs later after consumption, agreeing with T_{max} for Uro-A of ~36hrs after ingestion in a study of 16 healthy volunteers [19]. (3) For Uro-B, in volunteer no.1, trace concentration was detected at 8.5h after PE or PJ consumption. The occurrence of Uro-B was later than that of Uro-A, agreeing with the fact that Uro-B is the final product of microbial metabolism and is originated by removal of a hydroxyl group from Uro-A [21]. In contrast, Uro-B was undetectable in volunteer no.3. There are 2 potential explanations: one is that the generation rate of Uro-B is slower in this subject and Uro-B might be detected after 12 hours; the other one is that this subject might not be able to generate sufficient Uro-B to be detected in plasma.

Additionally, pharmacokinetic profiles might also depend on dosage forms. (1) For EA, in our results, PE and PJ trials showed different C_{max}; while T_{max} and AUC were similar. However, in another study, it was reported that T_{max} varied in different dosage forms, since T_{max} was determined as 0.65 ± 0.23hrs by the ingestion of pomegranate juice, 0.94 ± 0.06hrs by pomegranate liquid extract, while 2.58 ±

0.42hrs by pomegranate powder extract [19]. (2) For Uro-A, both 2 subjects in our study showed different profiles in PE and PJ trials. In volunteer no.11, the concentrations of Uro-A were slightly higher in PJ trial compared with PE trial. The differences in plasma concentrations might be explained by the different polyphenol content of intake (~800mg polyphenols in single-dose pomegranate juice vs. ~689mg polyphenols in single-dose pomegranate extract), or by the different dosage forms. However, in volunteer no.3, Uro-A (either free or glucuronide conjugated) was non-detectable in PE trial, while significantly elevated level of Uro-A glucuronide was detected in PJ trial. In this case, the different polyphenol content intake was not sufficient to explain these differences and the different dosage forms must be taken into consideration.

4.5 Further Directions

In the subsequent experiments, we will go through the samples from all the subjects, test the concentrations of 3 target analytes at all time points, generate the metabolic profiles and calculate the pharmacokinetic parameters. We will also compare pharmacokinetic profies between PE and PJ trials, to see whether different dosage forms might affect the absorption and elimination rate, and to compare the value of C_{max} or AUC between these two trials. To get a full pharmacokinetic profile of Uro-A and Uro-B, extended time points, more than 72hrs after administration, are needed. Since urolithins have favorable properties in vitro [4,47], a profile of major urolithins (Uro-A and Uro-B) would provide a valuable reference for understanding the clinical properties of pomegranate products.

References:

1. Gil MI, Tomas-Barberan FA, Hess-Pierce B, Holcroft DM, Kader AA (2000) Antioxidant activity of pomegranate juice and its relationship with phenolic composition and processing. J Agric Food Chem 48: 4581-4589.
2. Reddy MK, Gupta SK, Jacob MR, Khan SI, Ferreira D (2007) Antioxidant, antimalarial and antimicrobial activities of tannin-rich fractions, ellagitannins and phenolic acids from Punica granatum L. Planta Med 73: 461-467.
3. Velagapudi R, Baco G, Khela S, Okorji U, Olajide O (2015) Pomegranate inhibits neuroinflammation and amyloidogenesis in IL-1beta-stimulated SK-N-SH cells. Eur J Nutr.
4. Vicinanza R, Zhang Y, Henning SM, Heber D (2013) Pomegranate Juice Metabolites, Ellagic Acid and Urolithin A, Synergistically Inhibit Androgen-Independent Prostate Cancer Cell Growth via Distinct Effects on Cell Cycle Control and Apoptosis. Evid Based Complement Alternat Med 2013: 247504.
5. Medjakovic S, Jungbauer A (2013) Pomegranate: a fruit that ameliorates metabolic syndrome. Food Funct 4: 19-39.
6. Banerjee N, Kim H, Talcott S, Mertens-Talcott S (2013) Pomegranate polyphenolics suppressed azoxymethane-induced colorectal aberrant crypt foci and inflammation: possible role of miR-126/VCAM-1 and miR-126/PI3K/AKT/mTOR. Carcinogenesis 34: 2814-2822.
7. Vlachojannis C, Zimmermann BF, Chrubasik-Hausmann S (2015) Efficacy and safety of pomegranate medicinal products for cancer. Evid Based Complement Alternat Med 2015: 258598.
8. Poyrazoğlu E, Gökmen V, Artık N (2002) Organic Acids and Phenolic Compounds in Pomegranates (Punica granatum L.) Grown in Turkey. Journal of Food Composition and Analysis 15: 567-575.
9. Yang CS, Landau JM, Huang MT, Newmark HL (2001) Inhibition of carcinogenesis by dietary polyphenolic compounds. Annu Rev Nutr 21: 381-406.
10. Cerda B, Soto C, Albaladejo MD, Martinez P, Sanchez-Gascon F, et al. (2006) Pomegranate juice supplementation in chronic obstructive pulmonary disease: a 5-week randomized, double-blind, placebo-controlled trial. Eur J Clin Nutr 60: 245-253.
11. Pantuck AJ, Leppert JT, Zomorodian N, Aronson W, Hong J, et al. (2006) Phase II study of pomegranate juice for men with rising prostate-specific antigen following surgery or radiation for prostate cancer. Clin Cancer Res 12: 4018-4026.
12. Paller CJ, Ye X, Wozniak PJ, Gillespie BK, Sieber PR, et al. (2013) A randomized phase II study of pomegranate extract for men with rising PSA following initial therapy for localized prostate cancer. Prostate Cancer Prostatic Dis 16: 50-55.
13. Stenner-Liewen F, Liewen H, Cathomas R, Renner C, Petrausch U, et al. (2013) Daily Pomegranate Intake Has No Impact on PSA Levels in Patients with Advanced Prostate Cancer - Results of a Phase IIb Randomized Controlled Trial. J Cancer 4: 597-605.
14. Hanley MJ, Masse G, Harmatz JS, Court MH, Greenblatt DJ (2012) Pomegranate juice and pomegranate extract do not impair oral clearance of flurbiprofen in human volunteers: divergence from in vitro results. Clin Pharmacol Ther 92: 651-657.
15. Larrosa M, Garcia-Conesa MT, Espin JC, Tomas-Barberan FA (2010) Ellagitannins, ellagic acid and vascular health. Mol Aspects Med 31: 513-539.

16. Cerda B, Espin JC, Parra S, Martinez P, Tomas-Barberan FA (2004) The potent in vitro antioxidant ellagitannins from pomegranate juice are metabolised into bioavailable but poor antioxidant hydroxy-6H-dibenzopyran-6-one derivatives by the colonic microflora of healthy humans. Eur J Nutr 43: 205-220.
17. Larrosa M, Tomas-Barberan FA, Espin JC (2006) The dietary hydrolysable tannin punicalagin releases ellagic acid that induces apoptosis in human colon adenocarcinoma Caco-2 cells by using the mitochondrial pathway. J Nutr Biochem 17: 611-625.
18. Seeram NP, Henning SM, Zhang Y, Suchard M, Li Z, et al. (2006) Pomegranate juice ellagitannin metabolites are present in human plasma and some persist in urine for up to 48 hours. J Nutr 136: 2481-2485.
19. Seeram NP, Zhang Y, McKeever R, Henning SM, Lee RP, et al. (2008) Pomegranate juice and extracts provide similar levels of plasma and urinary ellagitannin metabolites in human subjects. J Med Food 11: 390-394.
20. Whitley AC, Stoner GD, Darby MV, Walle T (2003) Intestinal epithelial cell accumulation of the cancer preventive polyphenol ellagic acid--extensive binding to protein and DNA. Biochem Pharmacol 66: 907-915.
21. Espin JC, Larrosa M, Garcia-Conesa MT, Tomas-Barberan F (2013) Biological significance of urolithins, the gut microbial ellagic Acid-derived metabolites: the evidence so far. Evid Based Complement Alternat Med 2013: 270418.
22. Doyle B, Griffiths LA (1980) The metabolism of ellagic acid in the rat. Xenobiotica 10: 247-256.
23. Espin JC, Gonzalez-Barrio R, Cerda B, Lopez-Bote C, Rey AI, et al. (2007) Iberian pig as a model to clarify obscure points in the bioavailability and metabolism of ellagitannins in humans. J Agric Food Chem 55: 10476-10485.
24. Van Eeckhaut A, Lanckmans K, Sarre S, Smolders I, Michotte Y (2009) Validation of bioanalytical LC-MS/MS assays: evaluation of matrix effects. J Chromatogr B Analyt Technol Biomed Life Sci 877: 2198-2207.
25. Silvestro L, Tarcomnicu I, Savu SR (2013) Matrix Effects in Mass Spectrometry Combined with Separation Methods — Comparison HPLC, GC and Discussion on Methods to Control these Effects. Tandem Mass Spectrometry - Molecular Characterization.
26. Billett F (1954) The beta-glucuronidase of the Roman snail (Helix pomatia). Biochem J 57: 159-162.
27. Seeram NP, Lee R, Heber D (2004) Bioavailability of ellagic acid in human plasma after consumption of ellagitannins from pomegranate (Punica granatum L.) juice. Clin Chim Acta 348: 63-68.
28. Nunez-Sanchez MA, Garcia-Villalba R, Monedero-Saiz T, Garcia-Talavera NV, Gomez-Sanchez MB, et al. (2014) Targeted metabolic profiling of pomegranate polyphenols and urolithins in plasma, urine and colon tissues from colorectal cancer patients. Mol Nutr Food Res 58: 1199-1211.
29. Matuszewski BK, Constanzer ML, Chavez-Eng CM (2003) Strategies for the assessment of matrix effect in quantitative bioanalytical methods based on HPLC-MS/MS. Anal Chem 75: 3019-3030.
30. Cuadros-Rodriguez L, Bagur-Gonzalez MG, Sanchez-Vinas M, Gonzalez-Casado A, Gomez-Saez AM (2007) Principles of analytical calibration/quantification for the separation sciences. J Chromatogr A 1158: 33-46.
31. Kruve A, Herodes K, Leito I (2010) Optimization of electrospray interface and quadrupole ion trap mass

spectrometer parameters in pesticide liquid chromatography/electrospray ionization mass spectrometry analysis. Rapid Commun Mass Spectrom 24: 919-926.

32. API 2000 LC/MS/MS TurboIonSpray Ion Source Manual.
33. Sargent M, editor (2013) Guide to achieving reliable quantitative LC-MS measurements, RSC Analytical Methods Committee.
34. Yadav M, Patel D, Singhal P, Prasad R, Goswami S, et al. (2008) Effect of collision-activated dissociation gas and collision energy on the fragmentation of dipyridamole and its rapid and sensitive liquid chromatography/electrospray ionization tandem mass spectrometric determination in human plasma. Rapid Commun Mass Spectrom 22: 511-518.
35. Mertens-Talcott SU, Jilma-Stohlawetz P, Rios J, Hingorani L, Derendorf H (2006) Absorption, metabolism, and antioxidant effects of pomegranate (Punica granatum l.) polyphenols after ingestion of a standardized extract in healthy human volunteers. J Agric Food Chem 54: 8956-8961.
36. Hamad A-WR, Al-Momani WM, Janakat S, Oran SA (2009) Bioavailability of Ellagic Acid After Single Dose Administration Using HPLC. Pakistan Journal of Nutrition 8: 1661-1664.
37. Dams R, Huestis MA, Lambert WE, Murphy CM (2003) Matrix effect in bio-analysis of illicit drugs with LC-MS/MS: influence of ionization type, sample preparation, and biofluid. J Am Soc Mass Spectrom 14: 1290-1294.
38. Chambers E, Wagrowski-Diehl DM, Lu Z, Mazzeo JR (2007) Systematic and comprehensive strategy for reducing matrix effects in LC/MS/MS analyses. J Chromatogr B Analyt Technol Biomed Life Sci 852: 22-34.
39. Hall TG, Smukste I, Bresciano KR, Wang Y, McKearn D, et al. (2012) Identifying and Overcoming Matrix Effects in Drug Discovery and Development. In: Prasain J, editor. Tandem Mass Spectrometry - Applications and Principles.
40. King R, Bonfiglio R, Fernandez-Metzler C, Miller-Stein C, Olah T (2000) Mechanistic investigation of ionization suppression in electrospray ionization. J Am Soc Mass Spectrom 11: 942-950.
41. Yaroshenko DV, Kartsova LA (2014) Matrix Effect and Methods for Its Elimination in Bioanalytical Methods Using Chromatography–Mass Spectrometry. Journal of Analytical Chemistry 69: 311-317.
42. Mei H, Hsieh Y, Nardo C, Xu X, Wang S, et al. (2003) Investigation of matrix effects in bioanalytical high-performance liquid chromatography/tandem mass spectrometric assays: application to drug discovery. Rapid Commun Mass Spectrom 17: 97-103.
43. Unger S, Weng N (2013) Best Practice in Liquid Chromatography for LC-MS Bioanalysis. Handbook of LC-MS Bioanalysis: John Wiley & Sons Inc. pp. 185-204.
44. Polson C, Sarkar P, Incledon B, Raguvaran V, Grant R (2003) Optimization of protein precipitation based upon effectiveness of protein removal and ionization effect in liquid chromatography-tandem mass spectrometry. J Chromatogr B Analyt Technol Biomed Life Sci 785: 263-275.
45. Antignac J-P, de Wasch K, Monteau F, De Brabander H, Andre F, et al. (2005) The ion suppression phenomenon in liquid chromatography–mass spectrometry and its consequences in the field of residue analysis. Analytica Chimica Acta 529: 129-136.
46. King R, Bonfiglio R, Fernandez-Metzler C, Miller-Stein C, Olah T Mechanistic investigation of ionization suppression in electrospray ionization. Journal of the American Society for Mass Spectrometry 11: 942-950.

47. Gonzalez-Sarrias A, Larrosa M, Tomas-Barberan FA, Dolara P, Espin JC (2010) NF-kappaB-dependent anti-inflammatory activity of urolithins, gut microbiota ellagic acid-derived metabolites, in human colonic fibroblasts. Br J Nutr 104: 503-512.